SUPPLEMENTARY FIGURE LEGENDS

Figure S1. Gel electrophoresis assay of nucleosome array assembly. Related to Figures 2-4, and 6

Agarose gel electrophoresis of assembled nucleosome arrays. Arrays were prepared at different [histone octamers]:[601 DNA repeats] molar ratios (indicated above the gel image) as described in the "Nucleosome Assembly" section under Method Details. During nucleosome assembly, the 64mer DNA construct and 147 bp competitor DNA were mixed to an equal mass concentration of 35 ng/µL. For this agarose gel, 2 µL of the assembly was diluted in a Tris-EDTA buffer (10 mM Tris pH 8.0, 1 mM EDTA, 8% (v/v) glycerol) and loaded on a 0.7% agarose gel (6.5 x 10 cm). The gel was run under 15 V/cm in 0.2X TBE (Tris-borate-EDTA) buffer for 30 minutes and post-stained with ethidium bromide. As the assembly approached saturation, the mobility of the high molecular weight band was reduced and eventually plateaued, with concurrent formation of mono-nucleosomes assembled on the 147 bp competitor DNA. Because nucleosomes limit ethidium bromide staining of the bound DNA, the saturation of a nucleosome assembly is more readily assessed by the disappearance of competitor DNA (Dyer et al., 2004; Huynh et al., 2005).

Figure S2. Angular Optical Trap (AOT) capable of precision measurements for a broad range of substrate template length. Related to Figures 2-4.

Because a long DNA template of ~ 12.7 kbp was used in this study, torsional measurements must be performed over an extended axial distance (from 0 to 4 µm away from the coverslip)

on the AOT. Therefore, we optimized the AOT to allow for accurate torque measurements over this broad distance scale.

(A) Basic operational principle of the AOT. The AOT has enabled direct control and detection of torque and rotation in individual biomolecules. In an AOT, the trapped particle is a nanofabricated quartz cylinder that, when trapped, aligns its cylinder axis along the direction of light propagation (Deufel et al., 2007). When the incoming laser beam is linearly polarized with electric field $\vec{E}_{\mathrm{in}}$, the quartz cylinder develops a polarization $\vec{P}$ depending on the electric susceptibility $\overleftrightarrow{\chi}$ of the cylinder, which is anisotropic (χ_{e} along the extraordinary axis is greater than χ_{o} along the ordinary axes for quartz). The cylinder is fabricated so that the extraordinary axis is perpendicular to the cylinder axis. Once polarized, the cylinder will experience a torque τ analogous to that experienced by an electric dipole $\vec{p}$ in an electric field $\vec{E}$. This torque tends to align $\vec{p}$ to $\vec{E}$ and has a magnitude given by $\tau = \left|\vec{E} \times \vec{p}\right| = Ep\sin\theta$ where θ is the angle between $\vec{E}$ and $\vec{p}$. Though the equation for the torque on a cylinder is more complex due to its geometry (La Porta and Wang, 2004), the essential idea is the same. This torque will act until the extraordinary axis and $\vec{E}_{\mathrm{in}}$ are aligned, at which point $\vec{\tau} = 0$ since $\vec{E}$ is parallel to $\vec{p}$ and $\theta = 0$. The cylinder can thus be rotated about its axis by rotation of the laser polarization. Torsionally anchoring a biological molecule to one end of the cylinder allows the independent application of force and torque to the molecule. The torque that rotates the cylinder to align the extraordinary axis to the trapping laser's polarization is provided by the angular momentum intrinsically carried by light. Because angular momentum must be conserved, the torque imparted to the cylinder by the trapping laser can be detected via a change in the angular

momentum of the trapping laser after it passes through the trapped cylinder (La Porta and Wang, 2004). This is illustrated here by the change in the laser polarization from linear ($\vec{E}_{\mathrm{in}}$) to elliptical after it passes through the cylinder ($\vec{E}_{\mathrm{out}}$). The same trapping beam is thus used for torque application as well as the detection of the trapped particle's angle and the applied torque, without the need for a secondary detection beam or imaging method. This detection method is exceedingly direct, relying solely on conservation of angular momentum, and distinguishes the AOT from other torque detection methods.

(B) Experimental configuration to measure torque required to supercoil a DNA molecule. Here a DNA molecule was torsionally anchored at one end to a microscope coverslip and at the other end to the bottom of a trapped quartz cylinder. During a typical experiment, the force, displacement, torque, and angle of the cylinder are simultaneously measured at kilohertz frequencies as the cylinder is rotated to introduce supercoiling in the DNA (Deufel et al., 2007; Forth et al., 2008; Sheinin et al., 2011). In this work, the AOT has been optimized to allow for accurate measurements from long DNA substrates via rigorous torque calibrations to correct for spherical aberrations of trapping laser beam when it was focused into an aqueous medium.

(C) Direct torque measurements of a long DNA molecule. Shown are extension and torque measurements for naked DNA molecules of 12.7 kbp and 6.1 kbp in length. The experiments were conducted under 0.5 pN of force in the topoisomerase buffer. As twist was introduced to a DNA molecule, torque increased essentially linearly until the DNA buckled to form a plectoneme, after which the torque plateaued. Vertical dashed lines indicate buckling transitions. Because the torsional mechanics of DNA is scale invariant, torque versus

superhelical density should be independent of DNA length (Marko, 2007). Indeed, the measurements verified this within measurement uncertainty.

Figure S3. Single chromatin fiber composition, saturation, stability, and characteristics assayed using the angular optical trap (AOT). Related to Figures 2 and 3.

(A) Experimental configuration to stretch a chromatin fiber axially using the AOT. For each single chromatin fiber substrate investigated in Figure 3, immediately following the torsional measurement, the substrate was returned to the zero-turns state and then stretched along the axial direction of the AOT to disrupt nucleosomes (Figures 2B and 2C). The resulting force-extension curve allowed us to assay the composition of the nucleosome array (e.g., nucleosomes versus tetrasomes) and the number of nucleosomes on DNA.

(B) Nucleosome composition selection criterion. In the force-extension curve, an array containing only full nucleosomes and no tetrasomes should have $N_{\mathrm{in}} = N_{\mathrm{out}}$ (solid black line). A large deviation from this relation is indicative of an array with other nucleosomal structures. For example, an array containing some tetrasomes is expected to have $N_{\mathrm{in}} > N_{\mathrm{out}}$. We therefore impose a selection criterion that $\frac{|N_{\mathrm{in}} - N_{\mathrm{out}}|}{N_{in}} \leq 0.15$ with the selection boundary shown as a dash line. This criterion optimizes the chance of selecting a high quality array while accommodating measurement uncertainties in N_{in} and N_{out}. Each red dot came from a single trace that passed this selection criterion.

(C) Extension versus nucleosome array saturation relationships at 0.5 and 0.25 pN. During a twisting experiment, we intend to use the extension at zero turns to estimate the number of

nucleosomes on a substrate. Here, in order to establish this relationship using force versus extension curves, we examined this relation at two forces, 0.5 pN and 0.25 pN, for all arrays that passed the selection criteria shown in Figures S3B and S3E. The relationship at 0.5 pN was later used to estimate the number of nucleosomes on single chromatin fiber substrates in the experiments performed on MT. Similarly, the relationship at 0.25 pN was later used to estimate the number of nucleosomes on braided chromatin fiber substrates where the entire substrate was held at 0.5 pN, so that each array was expected to experience half of the total force assuming that the two arrays are parallel to each other. Error bars are SEMs.

(D) Experimental configuration to twist a single chromatin fiber substrate using the AOT.

(E) Single chromatin fiber stability under twisting. A selection criterion for a good array is that the extension versus turns relation (also known as the 'hat curve') must show sufficient stability and should be essentially reversible during the course of twisting measurements. Shown is an example trace of adding (black) and removing (red) turns, resulting in two hat curves. Data were smoothed by a 1 turn sliding window. We require that the average difference in extension between these two curves be < 50 nm.

(F) Characterizing buckling-like transitions in chromatin. To illustrate how the data analysis was performed to characterize buckling-like transitions of a single chromatin fiber, we make a sketch of the profile of a hat curve such as the one shown in (E). Each hat curve was fit by a 5-piecewise function, which consists of 3 linear regions (left, middle, and right linear, grey) and 2 quadratic regions (black). To reduce the size of the parameter space, we require that the function and its derivative be continuous. We define the position of a "buckling-like" transition

to be at the intercept of the fit to the middle linear region with that of an adjacent linear region. A useful quantity to characterize these transitions is the number of turns required for the onset of the transition in either the (-) or (+) direction. Here, we call this quantity the transition width: w_{t}^{-} for the (-) transition, and w_{t}^{+} for the (+) transition.

(G) The transition width as a function of the number of nucleosomes on DNA. Error bars are SEMs. The red lines are the linear fits to the data.

Figure S4. Braided chromatin fiber composition, saturation, stability, and characteristics assayed on the AOT. Related to Figures 2 and 4.

(A) Experimental configuration to stretch a double chromatin fiber substrate axially using the AOT. For each braided (double) chromatin fiber substrate investigated in main text Figure 4, we assayed the composition of the fibers and the level of saturation. Immediately following the torsional measurement, each substrate was returned to the zero-turns state and stretched along the axial direction of the AOT to disrupt nucleosomes in both arrays (Figures 2D and 2E).

(B) Nucleosome composition selection criterion. In the force-extension curve, if the two nucleosome arrays in a double substrate contain the same number of nucleosomes and only canonical nucleosomes, we expect that $N_{\mathrm{in}} = N_{\mathrm{out}}$ (black line). We impose a selection criterion that $\frac{|N_{\mathrm{in}} - N_{\mathrm{out}}|}{N_{in}} \leq 0.20$ (grey region). When the two arrays in a double substrate contain substantially different numbers of nucleosomes, our method for detecting the boundaries of inner-turn and outer-turn releases will result in a detected N_{in} closer to that of the array with a larger number of nucleosomes and the detected N_{out} closer to that of the array with a smaller

number of nucleosomes. Therefore, the detected $\frac{|N_{\mathrm{in}}-N_{\mathrm{out}}|}{N_{\mathrm{in}}}$ becomes large, so these substrates will naturally be excluded from further analysis. Thus this selection criterion simultaneously selects substrates with two arrays both being similar in the number of nucleosomes and containing primarily canonical nucleosomes. Each data point came from a single trace that passed this selection criterion.

(C) Experimental configuration to twist a double chromatin fiber substrate using the AOT. The distance of end anchor separation is also indicated.

(D) Stability of the braided chromatin fiber under twisting. Like the single chromatin fiber, a good braided chromatin substrate must show sufficient stability, and its hat curve should be reversible during the course of twisting measurements. Shown is an example trace of adding (black) and then removing (blue) turns, resulting in two hat curves. Data were smoothed by a 1 turn sliding window. We require that the average difference in extension between these two curves be < 50 nm.

(E) Hat height versus nucleosome array saturation for traces. As with a single chromatin fiber substrate, a convenient estimate for the number of nucleosomes on a braided chromatin fiber substrate may be obtained from the hat height (extension at 0 turns when the substrate is torsionally relaxed). In Figure S3C, we established the relationship of hat height as a function of the number of nucleosomes in an ideal braided chromatin fiber substrate where the two arrays contain the same number of nucleosomes and are parallel to each other. This ideal relationship is replotted here (black line). We then plotted measurements (blue dots) from braided fiber

substrates that passed the selection criteria shown in Figures S4B and S4D. We found that these measurements (blue dots) fall within 20% of the ideal value.

Figure S5. Braided chromatin substrate torsional stiffness measurements under twisting by the AOT. Related to Figure 4.

We intend to determine the torsional modulus of a braided chromatin fiber substrate from the torque versus turns relation of the AOT data (Figure 4C). Ideally these experiments should be performed with the end anchor separations of the two chromatin fibers resembling those during replication. Based on the dimensions of a replisome (Quantification and Statistical Analysis), we estimate that anchor separations are ~ 80 nm, much smaller than the overall length of chromatin substrates, which is on the order of a micron. Therefore, we need to develop a method to select traces with small anchor separations. Under the limit of zero anchor separations at both ends, the free energy to twist a braid is expected to change gradually, giving rise to smooth changes of both extension and torque near zero turns (Charvin et al., 2005). Therefore, the torsional modulus of the substrate can be determined via the slope of the torque versus turns relation. As anchor separations increase, the free energy to twist a braid is expected to vary abruptly between -0.5 and +0.5 turns, resulting in a sharp decrease in extension as well as overshoots and an apparent discontinuity in torque (Charvin et al., 2005).

In principle, traces with small anchor separations could be selected based on small torque overshoots and torque discontinuity. However, the noise in the torque signal limited the accuracy of this method of selection. Fortuitously, the extension signal, obtained concurrently

with the torque signal, had much lower noise and served as a better candidate for selection. We therefore selected traces with a smooth and rounded extension versus turns curve (hat curve) near zero turns using the following criteria. We first normalized each hat curve by its maximum extension and then fit the normalized extension data between -10 and +10 turns to a parabola. We require that the rise of the normalized extension above this fit be smaller than 0.015 and the quadratic term magnitude of the fit be smaller than $5 \times 10^{-4}/\text{turns}^2$. We estimate (Charvin et al., 2005) that the maximum rise limit of 0.015 corresponds to roughly ~ 130 nm in maximum anchor separations for arrays containing ~ 46 nucleosomes.

As shown in this figure, we found that upon this selection, the torque signal became more continuous without detectable overshoots. Nonetheless, it still exhibited a small torque discontinuity near zero turns. Thus, we fit the torque data at ≥ 3 turns to a linear function allowing for a torque intercept. The slope of this fit was then used as the torsional stiffness of a braid and converted to the torsional modulus (see Quantification and Statistical Analysis). This fitting function, instead of one with a zero-torque intercept, should provide a conservative estimate of the torsional modulus and avoid overstating our conclusions presented in the main text Figure 5.

(A) Naked DNA braiding. Data were smoothed using a sliding window of 0.02 turns for extension and 4 turns for torque. The blue curves are the same as shown in main text Figures 4B and 4C (gray curves) for traces that passed all selection criteria. The mean rise of the normalized extension above the fit was 0.010, corresponding to traces with smaller anchor separations. The red line is a fit to the blue torque data ≥ 3 turns, resulting in a slope of 0.17 ± 0.01 pN·nm/turn. The black curves represent an average of 8 traces with a mean rise of the

normalized extension above the fit of 0.040, corresponding to traces with larger anchor separations that did not pass the anchor separation selection criterion. As expected, at larger anchor separations, the extension showed a sudden decrease and the torque signal showed overshoots and a larger discontinuity near zero turns. In order to more clearly visualize the torque near zero turns, we show an inset for the black torque data smoothed to 0.02 turns. A fit to the black torque data ≥ 3 turns resulted in a slope of 0.15 ± 0.02 pN·nm/turn, comparable to that of the blue torque data, suggesting that this slope is insensitive to the selection criteria for the two sets of data analyzed here.

(B) Chromatin fiber braiding. The data were presented and processed in the same way as in (A), except for the use of chromatin substrates each containing 46 nucleosomes on average. The blue curves are the same as shown in main text Figures 4B and 4C (blue curves) for traces that passed all selection criteria. The mean rise of the normalized extension above the fit was 0.010, corresponding to traces with smaller anchor separations which are estimated to be ~ 70 nm (Charvin et al., 2005). The red line is a fit to the blue torque data ≥ 3 turns, resulting in a slope of 0.33 ± 0.03 pN·nm/turn. The black curves represent an average of 14 traces with a mean rise of the normalized extension above the fit 0.060, corresponding to traces with larger anchor separations that did not pass the selection criterion described above. Just as with naked DNA, at larger anchor separations, the extension showed a sudden decrease and the torque signal showed torque overshoots and a larger discontinuity near zero turns. A fit to the black torque data ≥ 3 turns resulted in a slope of 0.27 ± 0.09 pN·nm/turn, similar to the valued obtained from the blue torque data, again suggesting that this slope is insensitive to the anchor separation selection criteria for the two sets of data analyzed here.

Figure S6. Chromatin fiber integrity and saturation assayed on the MT. Related to Figure 6.

For substrates used for experiments on the MT shown in main text Figure 6, we also applied a selection process parallel to that used for experiments on the AOT. Unlike the AOT, the MT measures extension but not torque. Therefore, the selection criteria for data traces obtained using the MT must rely on the extension data only.

(A) Experimental configuration to twist a single chromatin fiber substrate using the MT.

(B) Single chromatin substrate stability. This experiment was conducted in a fashion similar to that for Figure S3E, except using the MT. We require that for a substrate to be used for further analysis, the average difference in extension between the curves of adding turns and removing turns be < 50 nm.

(C) Single substrate selection criterion based on (+) transition width w_t^+ versus number of nucleosomes. For each array, we also used the measured transition width in the (+) direction (w_t^+) versus number of nucleosomes as a selection criterion. The transition width is defined in Figure S3F. For each trace, we first estimated the number of nucleosomes based on the extension at zero turns using the relationship established in Figure S3C. Using this calculated number of nucleosomes, we then compared the measured w_t^+ with the expected value (solid black line, from Figure S3G). For an array to be selected for further analysis, we require that w_t^+ is within 20% of the expected value. This selection criterion takes into account errors in estimating the number of nucleosomes. The errors are in part due to difficulties in obtaining accurate measurements of the absolute extension on the MT.

(D) Experimental configuration to twist a double chromatin fiber substrate using the MT.

(E) Braided chromatin substrate stability. This experiment was conducted in a fashion similar to that for Figure S4D, except using the MT. We require that for a substrate to be used for further analysis, the average difference in extension between the curves of adding turns and removing turns be < 50 nm.

(F) Braided chromatin substrate selection for configuration with small anchor separations. We used a similar anchor separation selection method as that for the AOT data (Figure S5B). We require that the rise of the normalized extension above this fit be smaller than 0.07, and the quadratic term magnitude of the fit be smaller than $1.4 \times 10^{-3}/\text{turns}^2$. The blue curve represents a trace that passed this selection, indicative of having small anchor separations. Traces that passed this selection were used for analysis of Figure 6. We estimate (Charvin et al., 2005) that these traces have an average anchor separation of ~ 140 nm. On the other hand, the black curve did not pass this selection and shows a sharp peak near zero turns, indicative of large anchor separations.

Figure S1

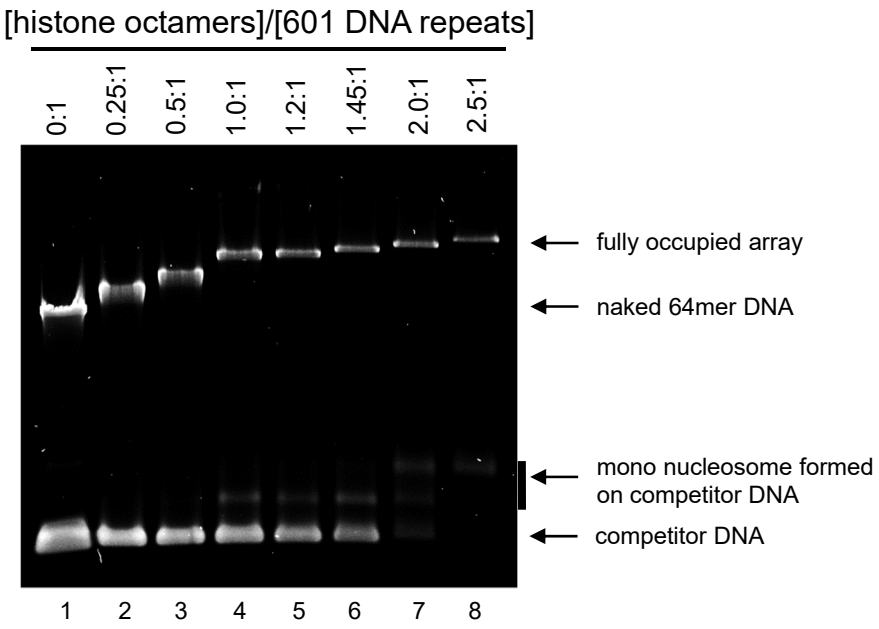

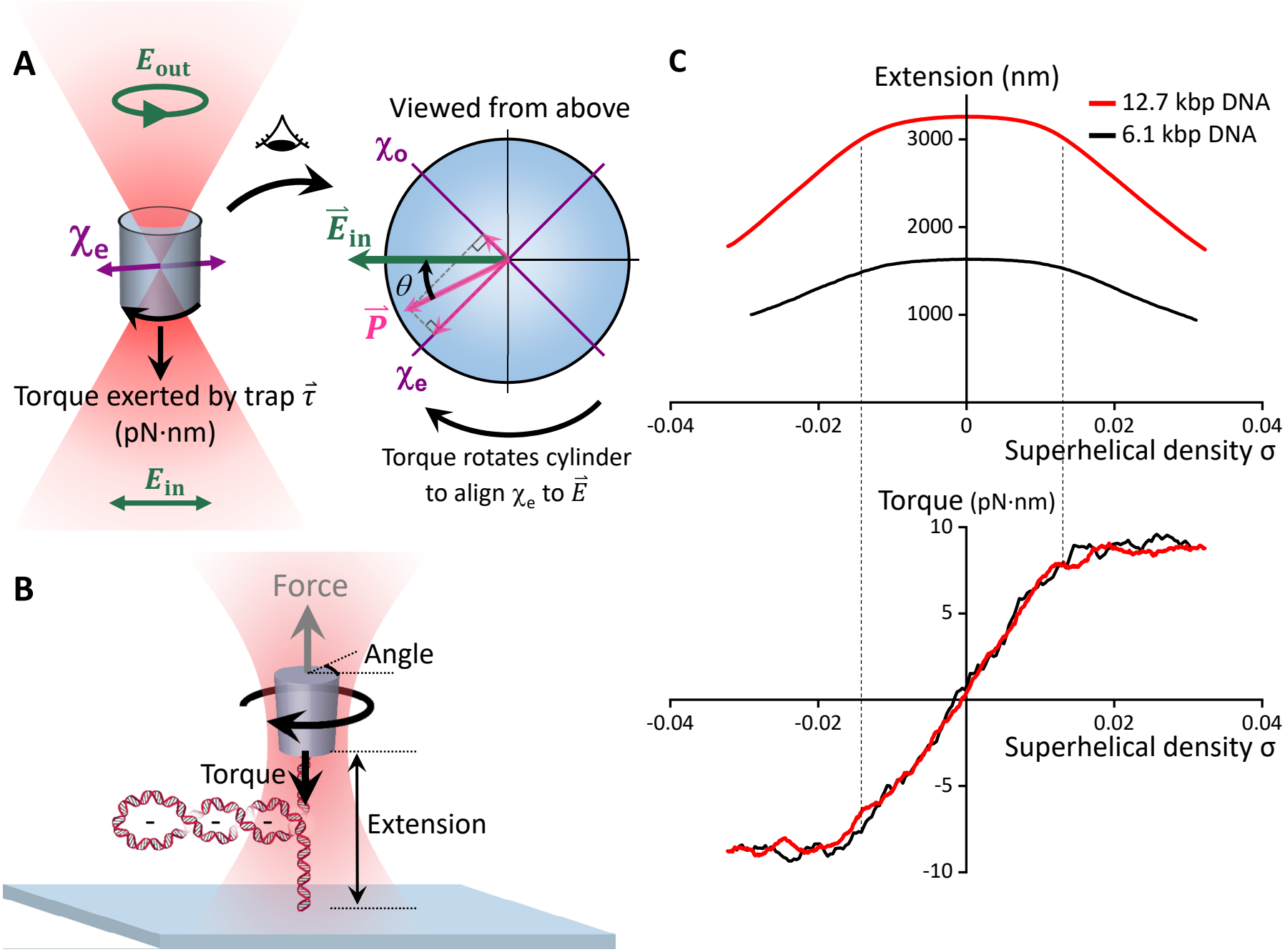

Figure S3

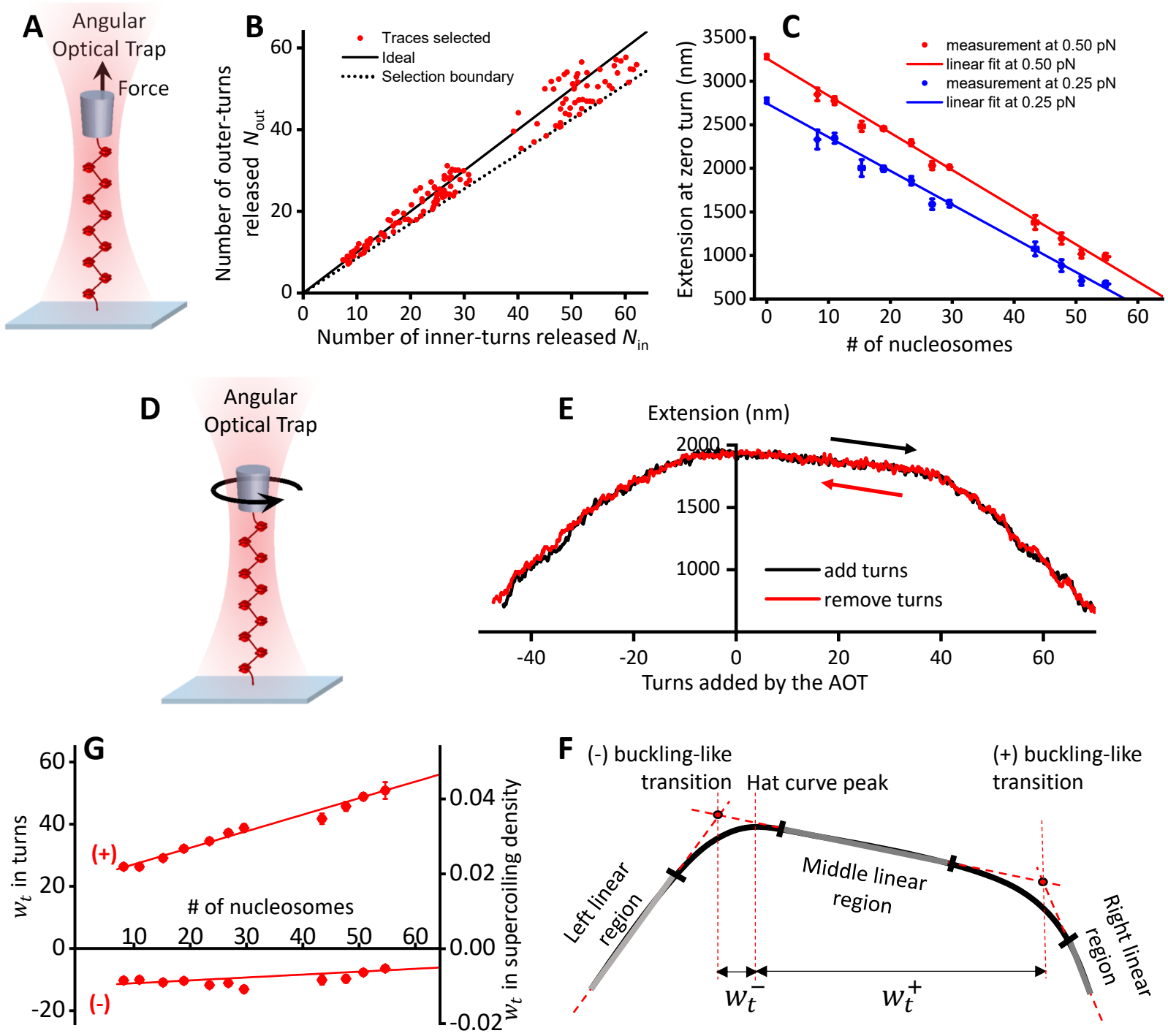

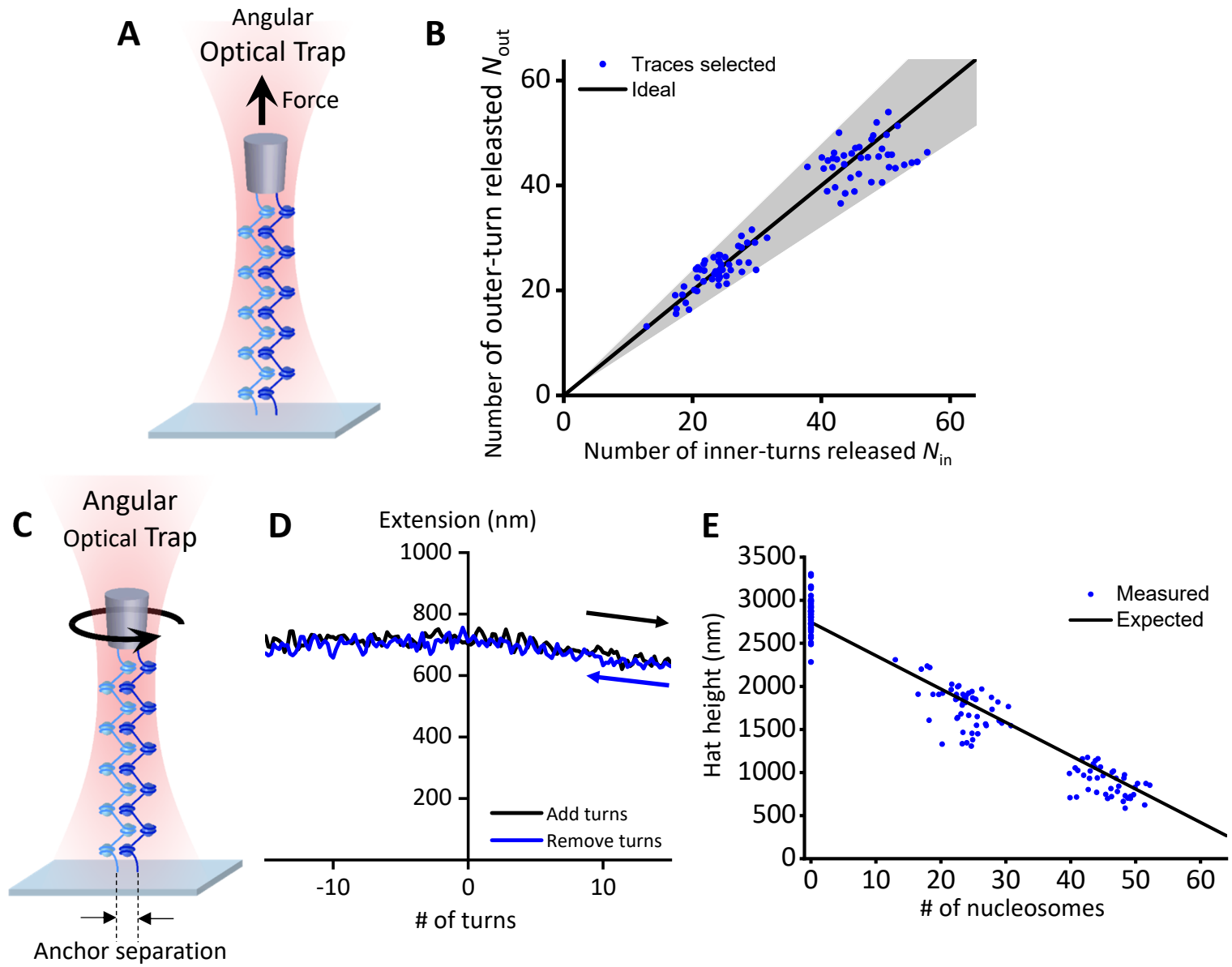

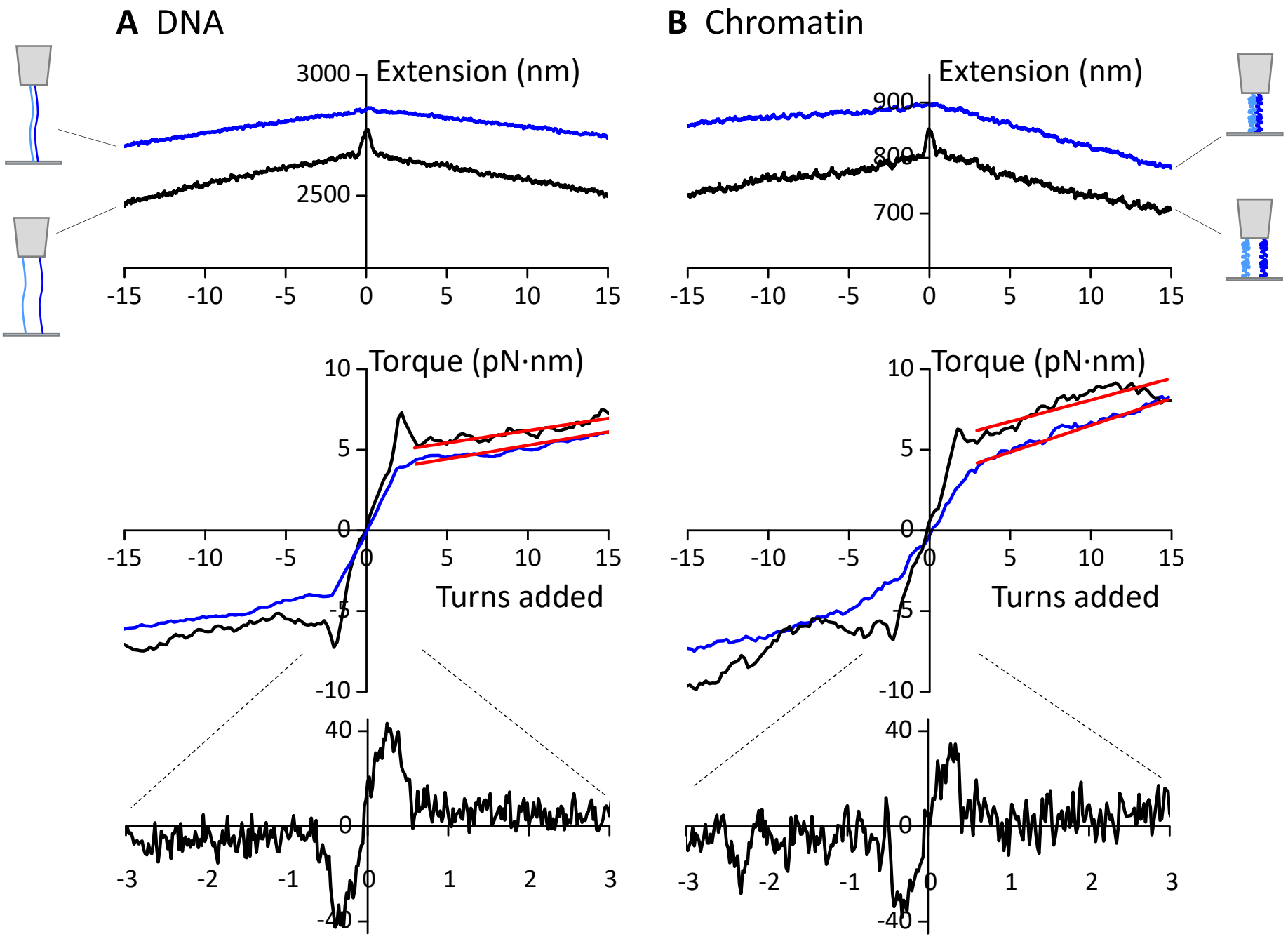

Figure S6